

Correction

IMMUNOLOGY AND INFLAMMATION.

Correction for “Cigarette smoke induces *miR-132* in Th17 cells that enhance osteoclastogenesis in inflammatory arthritis,” by Paula B. Donate, Kalil Alves de Lima, Raphael S. Peres, Fausto Almeida, Sandra Y. Fukada, Tarcilia A. Silva, Daniele C. Nascimento, Nerry T. Cecilio, Jhimmy Talbot, Rene D. Oliveira, Geraldo A. Passos, José Carlos Alves-Filho, Thiago M. Cunha, Paulo Louzada-Junior, Foo Y. Liew, and Fernando Q. Cunha, which published December 21, 2020; 10.1073/pnas.2017120118 (*Proc. Natl. Acad. Sci. U.S.A.* **118**, e2017120118).

The authors note that Fig. 3 appeared incorrectly. Specifically, the last panel of Fig. 3E inadvertently appeared as a duplicate of the second-to-last panel in Fig. 3C due to an error during figure compilation. The authors confirm that the corrected version was derived from data collected at the same time as the original experiments. The corrected figure and its legend appear below. The online version has been corrected.

Additionally, in the *SI Appendix*, page 8, second full paragraph, line 3, “($n = 5$ per group)” should instead appear as “($n = 4-6$ per group).” The *SI Appendix* has been corrected online.

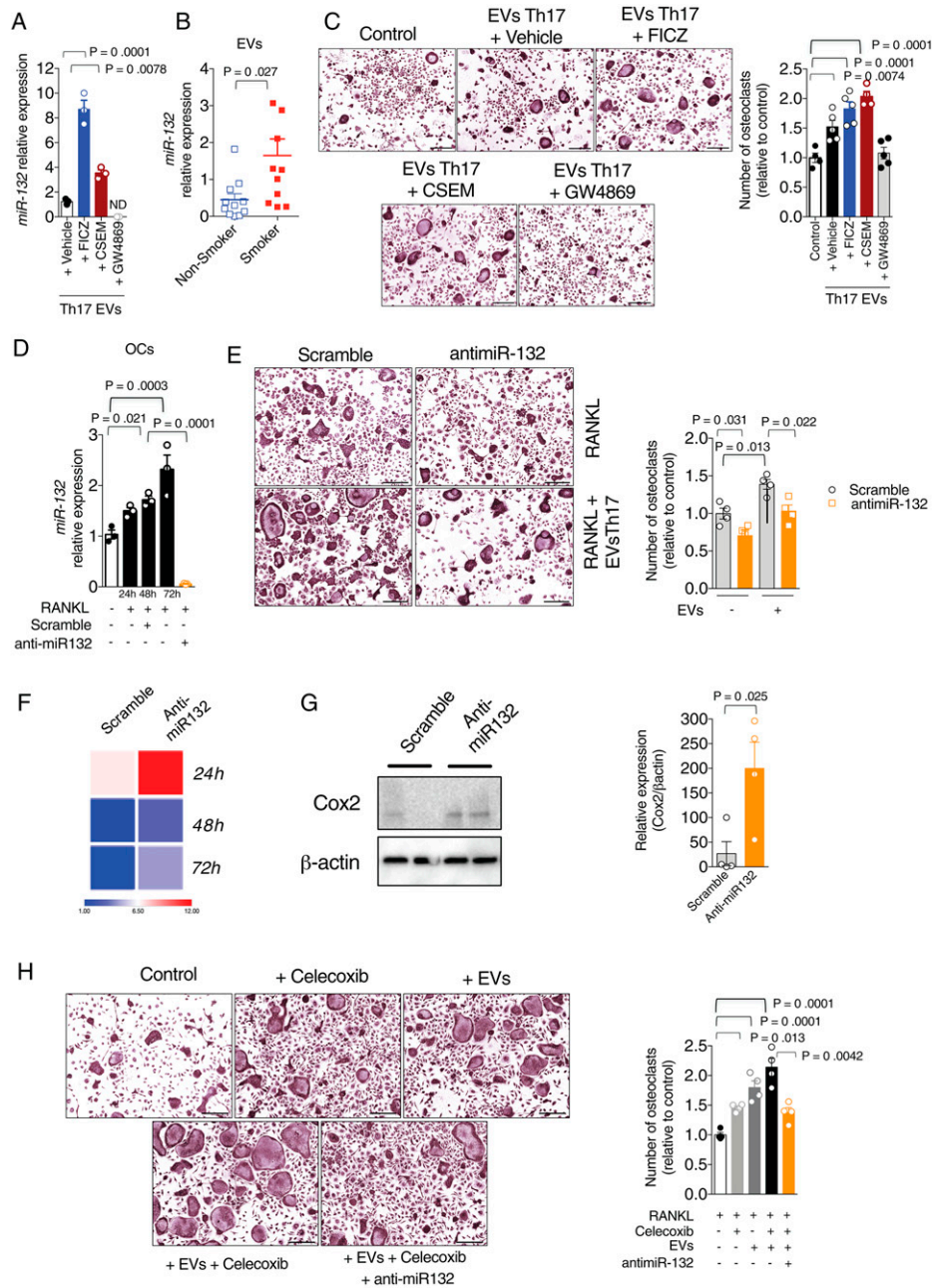


Fig. 3. AhR-induced *miR-132* is released by Th17 in extracellular vesicles and promotes osteoclastogenesis. Naive T cells ($CD4^+CD44^-CD62L^+$) were polarized to Th17 for 72 h (as in Fig. 1A) with or without FICZ, CSEM, or GW4869 (a vesicle-blocking agent). Culture supernatants were collected and EVs were isolated by ultracentrifugation. (A) Equal numbers of purified EVs were collected for qPCR analysis for *miRNA-132*. Statistical analysis was performed by one-way ANOVA followed by Bonferroni test. Data are representative of three independent experiments. ND, not detectable. (B) *miRNA-132* expression in EVs of the synovial fluids from nonsmoker ($n = 11$) and smoker ($n = 11$) RA patients. Results were calculated by the comparative threshold cycle method and are presented relative to that of *miR-361* (internal control miRNA). Statistical analysis was performed by nonparametric Mann-Whitney U test. (C) OCs were differentiated with RANKL and M-CSF in the presence of EVs from Th17 supernatants previously treated with vehicle, FICZ, CSEM, or GW4869. Images and number of TRAP⁺ multinuclear OCs are shown. (Scale bar, 75 μ m.) (D) *miR-132* expression during OC differentiation. (E) OCs were differentiated (as in C) in the presence of EVs from Th17 and transfected with anti-*miR-132* or scrambled control. Images and number of TRAP⁺ multinuclear OCs are shown. (Scale bar, 75 μ m.) (F) Heatmap of *Ptgs2* expression in OCs differentiated in the presence of anti-*miR-132* or scrambled control. (G) OCs collected after 72 h were analyzed by Western blot for the presence of COX2. Statistical analysis was performed by unpaired, two-tailed Student's t test. Data (mean \pm SEM) are from two independent experiments. (H) OCs were differentiated in the presence of RANKL and M-CSF for 48 h and then restimulated for 24 h with M-CSF and RANKL in the presence or absence of EVs isolated from Th17 pretreated with CSEM or a COX2 inhibitor, celecoxib. Some cells were also transfected with anti-*miR-132*. Representative images and number of multinuclear TRAP⁺ OCs are shown. (Scale bar, 75 μ m.) Statistical analysis was performed by one-way ANOVA followed by Bonferroni test or unpaired, two-tailed Student's t test ($n \geq 3$ /group). Data (mean \pm SEM) are representative of two independent experiments.

Published under the **PNAS** license.

Published October 18, 2021.

www.pnas.org/cgi/doi/10.1073/pnas.2117163118



Cigarette smoke induces *miR-132* in Th17 cells that enhance osteoclastogenesis in inflammatory arthritis

Paula B. Donate^a, Kalil Alves de Lima^a, Raphael S. Peres^a, Fausto Almeida^b, Sandra Y. Fukada^c, Tarcilia A. Silva^d, Daniele C. Nascimento^a, Nerry T. Cecilio^a, Jhimmy Talbot^a, Rene D. Oliveira^e, Geraldo A. Passos^f, José Carlos Alves-Filho^a, Thiago M. Cunha^a, Paulo Louzada-Junior^e, Foo Y. Liew^{g,1}, and Fernando Q. Cunha^{a,1}

^aDepartment of Pharmacology, Ribeirão Preto Medical School, University of São Paulo, Ribeirão Preto, SP, CEP 14049-900, Brazil; ^bDepartment of Biochemistry and Immunology, Ribeirão Preto Medical School, University of São Paulo, Ribeirão Preto, SP, CEP 14049-900, Brazil; ^cDepartment of BioMolecular Sciences, School of Pharmaceutical Sciences, University of São Paulo, São Paulo, SP, CEP 14040-903, Brazil; ^dDepartment of Oral Surgery and Pathology, School of Dentistry, Universidade Federal de Minas Gerais, Belo Horizonte, MG, CEP 31270-901, Brazil; ^eDepartment of Internal Medicine, Ribeirão Preto Medical School, University of São Paulo, Ribeirão Preto, SP, CEP 14049-900, Brazil; ^fMolecular Immunogenetics Group, Department of Genetics, Ribeirão Preto Medical School, University of São Paulo, Ribeirão Preto, SP, CEP 14049-900, Brazil; and ^gDivision of Immunology, Infection and Inflammation, Glasgow Biomedical Research Centre, University of Glasgow, Glasgow G12 8TA, United Kingdom

Edited by Marc Feldmann, University of Oxford, Oxford, United Kingdom, and approved November 18, 2020 (received for review August 15, 2020)

Rheumatoid arthritis (RA) is a chronic inflammatory disease characterized by joint destruction and severe morbidity. Cigarette smoking (CS) can exacerbate the incidence and severity of RA. Although Th17 cells and the Aryl hydrocarbon receptor (AhR) have been implicated, the mechanism by which CS induces RA development remains unclear. Here, using transcriptomic analysis, we show that *microRNA-132* is specifically induced in Th17 cells in the presence of either AhR agonist or CS-enriched medium. *miRNA-132* thus induced is packaged into extracellular vesicles produced by Th17 and acts as a proinflammatory mediator increasing osteoclastogenesis through the down-regulation of COX2. In vivo, articular knockdown of *miR-132* in murine arthritis models reduces the number of osteoclasts in the joints. Clinically, RA patients express higher levels of *miR-132* than do healthy individuals. This increase is further elevated by cigarette smoking. Together, these results reveal a hitherto unrecognized mechanism by which CS could exacerbate RA and further advance understanding of the impact of environmental factors on the pathogenesis of chronic inflammatory diseases.

cigarette smoke | rheumatoid arthritis | Th17 | exosomes | osteoclastogenesis

Rheumatoid arthritis (RA) is a chronic autoimmune disorder that affects about 1% of the adult population and is characterized by synovial inflammation and bone destruction, eventually leading to disability (1, 2). The interaction of several genes with environmental and stochastic factors controls the onset and development of the disease (3).

Cigarette smoke (CS), a key environmental factor, is highly associated with RA risk and mediates an increase of proinflammatory cytokine levels, affecting disease activity (4, 5). CS contains agonists for AhR (6–8). We have previously demonstrated a critical role of AhR on Th17 cells in arthritis development, which is exacerbated by CS (9). While wild-type (WT) mice developed exacerbated inflammatory arthritis and elevated frequency of CD4⁺IL-17⁺ T cells in the draining lymph nodes (DLN) when exposed to CS, AhR^{-/-} mice did not. Furthermore, an AhR antagonist (CH223191) also blocked the effect of CS in the WT mice (9). However, the molecular mechanism involved in this process is not fully understood.

AhR belongs to the helix–loop–helix Per-Arnt-Sim (bHLH-PAS) domain transcription factor family, well known for its response to various external stimuli and regulation of the immune system (10–12). In experimental models of arthritis and clinical RA, AhR activation induces proinflammatory cytokine production by different cell types, including Th17, fibroblasts, and synoviocytes (13, 14). AhR is also important for maintaining Th17 cell polarization (11, 15–17), characterized by the induction of *RORγt*

and *CYP11A1* and the production of interleukin-17 (18), which plays an important role in RA pathogenesis (19, 20).

CS is also significantly associated with epigenetic modification. The microRNAs (miRNAs), a class of small noncoding single-stranded RNA with posttranscriptionally regulatory properties (21, 22), play important roles in pathological conditions including RA (23–25). However, the relationship between AhR activation via CS, microRNA, and RA pathogenesis is unknown.

In this report, we demonstrate that the transcription of *miR-132*, activated by CS-induced AhR activation in Th17 cells, enhances osteoclastogenesis and contributes to the development and progression in experimental RA and clinical RA. The *miR-132* is packaged in extracellular vesicles (EVs) and mediates osteoclastogenesis by the down-regulation of *Ptsg2* expression and COX2 transcription. These results therefore provide a hitherto unrecognized mechanism by which CS could exacerbate local inflammation and joint destruction in RA. Understanding this linkage may provide a key mechanism by which CS exacerbates inflammation in general.

Significance

This report reveals a mechanism by which cigarette smoke (CS) could exacerbate local inflammatory disease. CS is a key environmental pollutant affecting millions of people globally and continues to be of considerable interest to the biomedical communities. We found that CS activates the AhR on Th17 cells, leading to the up-regulation of *miR-132*, which is then packaged into extracellular vesicles that induce osteoclastogenesis via the suppression of *Cox2* that catalyzes prostaglandins. Clinically, rheumatoid arthritis (RA) patients who smoke express a higher level of *miRNA-132* compared to nonsmoking RA patients. This finding not only reveals a mechanism of CS signaling but also may provide a potential target for therapeutic intervention for inflammatory disease in general and RA in particular.

Author contributions: P.B.D., S.Y.F., T.A.S., R.D.O., J.C.A.-F., T.M.C., P.L.-J., F.Y.L., and F.Q.C. designed research; F.Y.L. and F.Q.C. supervised the project; P.B.D., K.A.d.L., R.S.P., F.A., D.C.N., N.T.C., and J.T. performed research; G.A.P. contributed new reagents/analytic tools; P.B.D., K.A.d.L., R.S.P., F.A., S.Y.F., T.A.S., D.C.N., N.T.C., J.T., R.D.O., J.C.A.-F., T.M.C., P.L.-J., F.Y.L., and F.Q.C. analyzed data; and P.B.D., F.Y.L., and F.Q.C. wrote the paper.

The authors declare no competing interest.

This article is a PNAS Direct Submission.

Published under the PNAS license.

¹To whom correspondence may be addressed. Email: f.y.liew@clinmed.gla.ac.uk or fdqcunha@fmrp.usp.br.

This article contains supporting information online at <https://www.pnas.org/lookup/suppl/doi:10.1073/pnas.2017120118/-DCSupplemental>.

Published December 28, 2020.

Results

AhR Activation Induces Expression of a Specific microRNA Set in Th17 Cells. We first investigated whether AhR activation could affect miRNA expression in Th17 cells. Naive T cells ($CD4^+CD44^-CD62L^+$) were purified from the lymph nodes of C57BL/6 mice and polarized to Th17 cells in vitro in the presence of IL-6, TGF- β , and IL-1. After 72 h, IL-17-producing cells were purified and restimulated for 24 h with IL-6, TGF- β , IL-1, and IL-23 in the presence or absence of FICZ (6-formylindolo[3,2-b]carbazole, a well-documented AhR agonist). Th0 condition was used as a control, and isolated $CD4^+$ T cells were restimulated with IL-2 in the presence or absence of FICZ. Supervised hierarchical clustering analysis identified 224 differentially expressed miRNAs (fold-change ≥ 2.0 and false discovery rate [FDR] $< 5\%$). Among them, 22 miRNAs were up-regulated in Th17 cells in the presence of FICZ (Fig. 1A and *SI Appendix, Table S1*).

We then matched miRNA homology between humans and mice and selected two of the most expressed miRNAs after AhR activation, *miR-132* and *miR-346* (Fig. 1B), for validation by quantitative PCR (qPCR). We selected these two miRNAs based on their high level of expression and potential clinical relevance. FICZ markedly increased the expression of these two miRNAs in Th17 cells (Fig. 1C). AhR activation by FICZ also increased the expression of *Cyp1a* (the AhR downstream reporter gene) (Fig. 1D), IL-17A (Fig. 1E), and IL-22 production (Fig. 1F). These results demonstrate that AhR activation in Th17 cells induces the expression of *miRNA-132* and *miR-346*, which are highly homologous in mice and humans.

AhR-Induced *miR-132* and *miR-346* Are Correlated with Arthritis Development. Next, we explored whether AhR-induced *miR-132* and *miR-346* expression is associated with the development of inflammatory arthritis using the well-defined murine arthritic models, antigen-induced arthritis (AIA) and collagen-induced arthritis (CIA). In the AIA model, WT and *Ahr*^{-/-} C57BL/6 mice were primed and boosted with methylated bovine serum albumin (mBSA) and injected intraperitoneally with FICZ or vehicle alone. As demonstrated earlier (9), inflammatory arthritis was markedly exacerbated by the treatment with FICZ in the WT mice, whereas *Ahr*^{-/-} mice showed a minimal level of disease, which was not affected by the treatment of FICZ. While the expression of *miR-132* and *miR-346* in the Th17 cells from the lymph nodes of the WT mice was significantly enhanced by the treatment of FICZ, the low level of expression of these miRNAs in the Th17 cells of the *Ahr*^{-/-} mice was not affected by the treatment of FICZ (Fig. 2A). In the CIA model, DBA/1J mice were primed and boosted with type II collagen and treated intraperitoneally with FICZ or vehicle. As FICZ exacerbated the inflammatory arthritis (9), the treatment also significantly increased the expression of *miR-132* and *miR-346* in the Th17 cells from the lymph nodes of the CIA mice (Fig. 2B).

CS contains a variety of AhR agonists (7, 8). We therefore explored the effect of CS on miRNA expression in both AIA and CIA mice exposed to CS during the development of arthritis. As expected, CS exposure significantly exacerbated the inflammatory arthritis (*SI Appendix, Fig. S1*). CS markedly increased the expression of *miR-132* and *miR-346* in the Th17 cells from the lymph nodes of AIA mice (Fig. 2C). Supporting this observation, CS also enhanced the expression of *Cyp1a1* (Fig. 2C). Similarly, CS enhanced the expression of these two miRNAs in the Th17 cells from the lymph nodes of the CIA mice (Fig. 2D). Together, these results demonstrate that AhR activation leads to increased expression of *miR-132* and *miR-346* in the Th17 cells during inflammatory arthritis.

Increased Expression of miRNAs in Clinical RA. We next investigated the relevance of the specific expression of *miR-132* and *miR-346*

in RA patients. We recruited 37 untreated RA patients and 34 matched healthy individuals (*SI Appendix, Table S2*). $CD4^+$ T cells from the peripheral blood of the RA patients expressed significantly higher levels of human *miR-132* and *miR-346* compared to the cells from the healthy controls (Fig. 2E). We then stratified the RA patients as nonsmokers ($n = 18$) and smokers ($n = 19$). $CD4^+$ T cells from the smoker RA patients expressed a significantly higher level of *miR-132* than that of the cells from the nonsmokers (Fig. 2F). This was accompanied by a higher level of expression of *CYP1A1* in the T cells from the smokers compared to that of the nonsmokers. Strikingly, there was no significant difference in the expression of *miR-346* between the T cells from the smoker and nonsmoker RA patients (Fig. 2F). These results indicate that the data obtained from the experimental murine models of inflammatory arthritis may be applicable to clinical RA. Since the differential expression of *miR-346* was not obvious in the T cells between the smoker and nonsmoker RA patients, we focused our investigation on the functional role of *miR-132*.

AhR-Induced *miR-132* Is Released in EVs by Th17 Cells. We then investigated the effect of the AhR-induced increase in *miR-132* expression on the function of Th17 cells. Murine naive T cells ($CD4^+CD44^-CD62L^+$) were purified from the lymph node of WT C57BL/6 mice and polarized to Th17 cells with or without FICZ. The cells were also transfected with anti-*miR-132* or scrambled anti-*miR*. *miR-132* expression was significantly blocked by anti-*miR-132*, demonstrating the efficacy of the transfection (*SI Appendix, Fig. S2A*). However, blocking of *miR-132* had no effect on the differentiation of Th17 cells as shown by the percentage of $CD4^+$ cells positive for IL-17A, IFN γ , or IL-17A/IL-22 (*SI Appendix, Fig. S2B*). *miR-132* also had no effect on established Th17 cells, as transfection of polarized Th17 with anti-*miR-132* had no influence on the percentage of $CD4^+$ cells expressing IL-17A and IL-17A/IL-22 in the polarized Th17 cells (*SI Appendix, Fig. S2C*).

We then explored the possible effects of *miR-132* on other Th17 cell functions. EVs are an important mechanism of intercellular communication (26). EVs can carry and selectively deliver bioactive molecules such as miRNAs and modulate the activities of receptor cells (27). We therefore explored the possibility that the AhR-induced *miR-132* could be packaged and released to exert its functions on target cells.

Using a series of ultracentrifugation steps, we first purified, characterized, and extracted RNA of EV pellets from the supernatants of naive T cells cultured under the Th17 condition. Nano-tracking analysis revealed an average-size distribution of 123 nm, indicating that Th17 cells are releasing exosomes. We then investigated the potential role of EVs in the function of AhR-activated Th17 in the context of inflammatory arthritis. Naive $CD4^+$ T cells were sorted from the lymph nodes of C57BL/6 mice and polarized to Th17 in the presence of FICZ. In some cultures, we also added cigarette smoke-enriched medium (CSEM). CSEM has been shown to be a surrogate for CS in in vitro culture (9). CSEM was able to enhance Th17 differentiation and increased the expression of *miR-132* (*SI Appendix, Fig. S3*). Activation of AhR by either FICZ or CSEM did not significantly affect EV formation during the Th17 differentiation in vitro (*SI Appendix, Fig. S4A*). Th17-derived EV zeta potential ranged from an average of -8.05 for control cultures to -9.38 after AhR activation. These values suggest that only the contents of the vesicles could be altered by the receptor activation. Western blot analysis shows that the EV markers tetraspanin CD63 and Argo2 (involved in microRNA biogenesis) were detected in the EV preparations derived from the Th17 cells (*SI Appendix, Fig. S4B*).

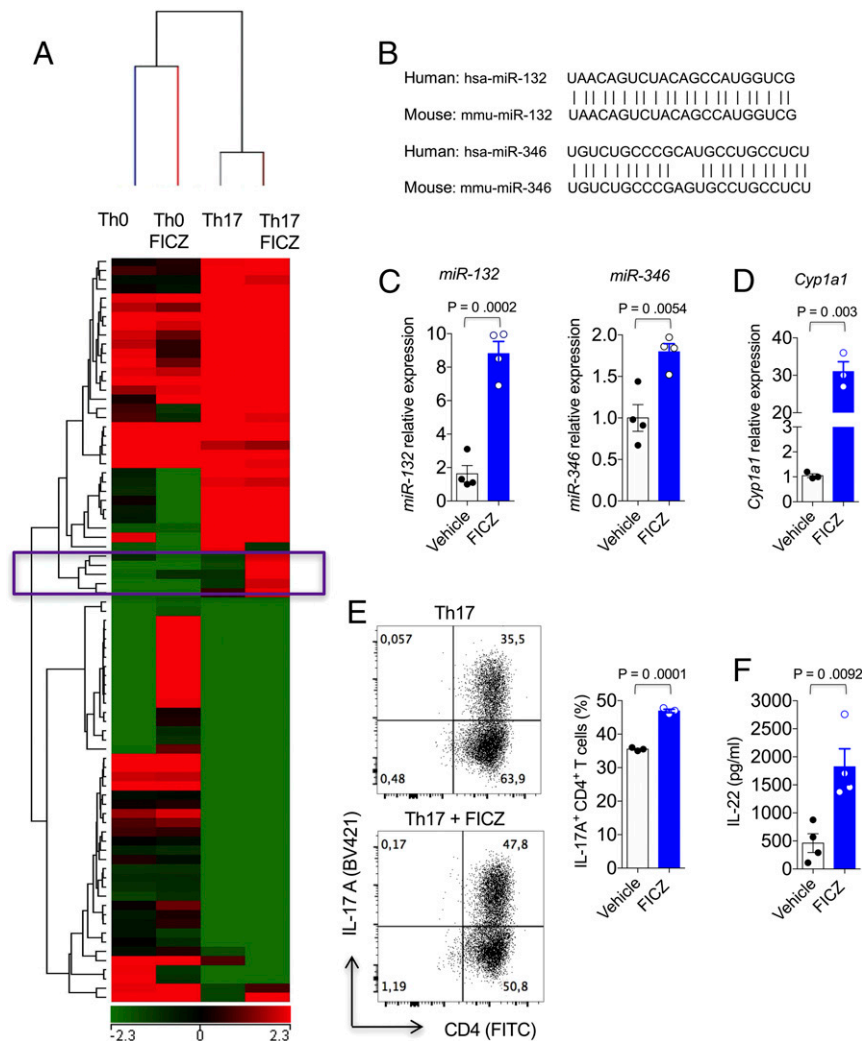


Fig. 1. AhR activation induces the expression of specific miRNAs in Th17 cells. Naive T cells ($CD4^+CD44^-CD62L^+$) were activated with plate-bound anti-CD3 and soluble anti-CD28, and polarized to Th17 with a mixture of TGF- β 1, IL-6, and IL-1 β for 72 h. (A) Heatmap of miRNA significantly expressed (fold-change ≥ 2.0 and FDR $< 5\%$) in IL-17-producing $CD4^+$ T cells cultured for a further 24 h with the cytokine mixture plus IL-23 with or without FICZ. $CD4^+$ T cells cultured in the presence of IL-2 were used as control (Th0). (B) miRNA homologous sequences between mice and humans obtained from miRBase. qPCR analysis of (C) *miR-132*, *miR-346*, and (D) *Cyp1a1* in Th17 cells. Results were calculated by the comparative threshold cycle method. (E) Representative dot plot of $CD4^+$ IL-17A $^+$ T cell frequency assessed by flow cytometry and frequency of $CD4^+$ IL-17A $^+$ T cells. (F) An enzyme-linked immunosorbent assay of IL-22 in the supernatants of Th17 cell differentiation as in E. Data are mean \pm SEM, representative of three independent experiments. Statistical analysis was performed by unpaired, two-tailed Student's *t* test ($n \geq 3$ /group).

We next investigated whether AhR activation of Th17 cells could affect the expression of *miR-132* in the EVs secreted by the Th17 cells. Murine $CD4^+$ T cells were polarized under the Th17 condition in the presence of FICZ, CSEM, or GW4869 (an inhibitor of EVs). Equal numbers of EVs were collected from the culture supernatant from each treatment, and the level of *miR-132* expression was determined by qPCR. FICZ and CSEM significantly increased the expression of *miR-132* in the EVs (Fig. 3A). The expression of *miR-132* was completely abolished in the presence of GW4869.

To determine the clinical relevance of this observation, we collected the synovial fluid from 11 smoker and 11 nonsmoker RA patients. EVs were harvested from the fluids and analyzed for the expression of *miR-132* by qPCR. The EVs from the smoker RA patients expressed significantly higher levels of *miR-132* than those from the nonsmoker RA patients (Fig. 3B). Together, these results demonstrate that AhR-induced *miR-132* in the EVs is closely associated with the inflammatory arthritis in mice and humans.

EVs from Th17 Cells Induce Osteoclastogenesis. The possibility that Th17-derived EVs could contribute to the inflammatory process in arthritis by acting on other immune cells was then explored. Mouse bone-marrow-derived dendritic cells were cultured with lipopolysaccharide (LPS) with or without EVs from Th17. The EVs had no effect on the DC number or the cytokines (TNF, IL-6, IL-23) produced (SI Appendix, Fig. S5A). Bone marrow-derived macrophages were also cultured under M0 (medium alone), M1 (LPS), or M2 (IL-4) conditions with or without Th17 EVs. The EVs again had no effect on the polarization of macrophages (SI Appendix, Fig. S5B).

Next, we tested the effect of Th17 EVs on osteoclastogenesis. Murine bone-marrow-derived preosteoclasts (pre-OCs) were cultured with RANKL/M-CSF in the presence or absence of Th17-derived EVs, and the resulting number of TRAP $^+$ multinucleated cells was determined. The number of osteoclasts (OC) was significantly increased by the presence of EVs from Th17 cells. This number was further elevated by the EVs from Th17

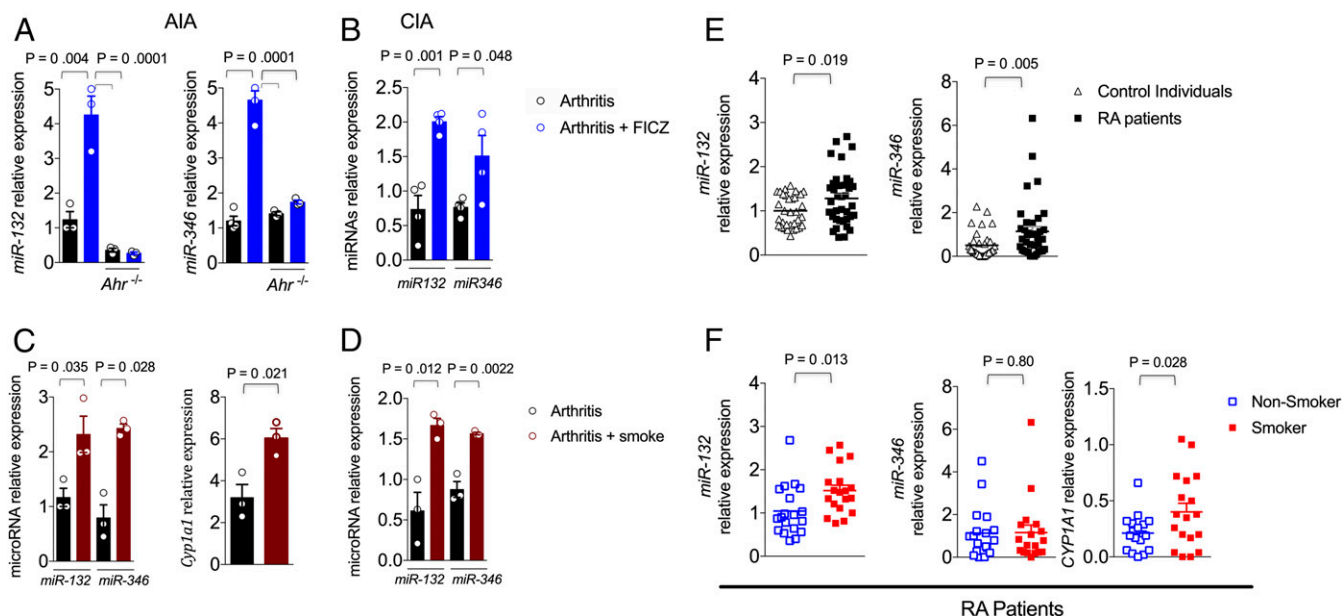


Fig. 2. Ahr activation-induced miRNAs are associated with arthritis. qPCR for *miR-132* and *miR-346* expression in CD4⁺ IL-17⁺ T cells isolated from draining lymph nodes of (A) WT C57BL/6 or Ahr-deficient mice in the AIA model and (B) DBA-1/J mice in the CIA model. Mice were treated with FICZ or vehicle (dimethylsulfoxide). (C) *miR-132*, *miR-346*, and *Cyp1a1* expression in AIA mice exposed or not to cigarette smoke during immunization. (D) miRNA expression in CIA mice exposed or not to cigarette smoke as in C. Data are representative of three independent experiments, and IL-17⁺ cells were pooled from three mice (mean ± SEM). Results were calculated by the comparative threshold cycle method. Statistical analysis was performed by one-way ANOVA followed by Bonferroni test or unpaired two-tailed Student's *t* test ($n \geq 3$ /group). (E and F) CD4⁺ T cells were isolated from the peripheral blood of RA patients ($n = 37$) or healthy controls ($n = 34$). Total RNA was extracted for qPCR analysis. (E) Expression of *miR-132* and *miR-346* in the T cells from controls and RA patients. (F) *miR-132*, *miR-346*, and *CYP1A1* expression in the T cells from nonsmoker ($n = 18$) and smoker ($n = 19$) RA patients. Results were calculated by the comparative threshold cycle method and are presented relative to that of *RNU48* (internal control miRNA) or *GAPDH* (internal control). Statistical analysis was performed by nonparametric Mann-Whitney *U* test.

cells previously cultured with FICZ or CSEM. However, these increases were blocked by the presence of GW4869 (Fig. 3C).

To confirm the role of *miR-132* in osteoclastogenesis, murine bone marrow pre-OCs were differentiated to OC in the presence of RANKL and M-CSF, and the level of *miR-132* expression was followed over a 72-h period. Some of the OC were transfected with anti-*miR-132* or its scrambled control. The expression of *miR-132* in the OC increased steadily over 72 h of culture. This expression was completely blocked by the transfection of anti-*miR-132* (Fig. 3D). We then differentiated pre-OCs with RANKL/M-CSF in the presence or absence of EVs from Th17 cells and transfected the OC with anti-*miR-132* or the scrambled control. The anti-*miR-132* effectively blocked the differentiation of OC by RANKL/M-CSF alone or in combination with Th17 EVs (Fig. 3E). These results therefore demonstrate that Th17 cells increase osteoclastogenesis by *miR-132* delivered to the pre-OCs via EVs.

miR-132 Inhibits Cox2 Induction during OC Differentiation. We then explored the mechanism by which *miR-132* induces osteoclastogenesis. A recent report suggested that *miR-132* could down-regulate the expression of the *prostaglandin-endoperoxide synthase 2* (*PTGS2*) gene during human macrophage-OC differentiation (28). *PTGS2* encodes the enzyme cyclooxygenase 2 (COX2), which catalyzes critical steps in the synthesis of prostaglandins (PGs) from arachidonic acid. PGE₂, PGD₂, and PGF₂ are reported to have inhibitory effects on OC function (29–33). We therefore investigated the role of *Ptgs2* and COX2 in the induction of osteoclastogenesis by EVs from Th17 cells. Murine pre-OC was cultured with RANKL/M-CSF in the presence of anti-*miR-132* or scrambled control. The expression of the *Ptgs2* gene was progressively reduced during OC differentiation in a time-dependent manner, and this was reversed by the

presence of anti-*miR-132* (Fig. 3F). This result was confirmed by Western blot analysis for the level of COX2 in the differentiated OC. COX2 protein level was significantly elevated in the OC by the transfection of anti-*miR-132* (Fig. 3G). We then tested the effect of celecoxib (a well-defined COX2 inhibitor) on osteoclastogenesis. Pre-OCs were cultured with RANKL/M-CSF in the presence of celecoxib, EVs, or anti-*miR-132*. The number of OC was significantly increased by the blocking of COX2 with celecoxib, and this increase was further elevated by the presence of the EVs of Th17 previously cultured with CSEM (Fig. 3H). Strikingly, the increase in the number of OC was inhibited by the presence of anti-*miR-132* (Fig. 3H). These results show that the *Ptgs2*-*Cox2* pathway plays an important role in the *miR-132*-induced OC differentiation mediated by Th17 cell EVs activated by CS.

Anti-*miR-132* Blocks Arthritis and Osteoclastogenesis In Vivo. To determine the role of *miR-132* in osteoclastogenesis in vivo, C57BL/6 mice were primed and boosted with mBSA (AIA model) and injected intra-articularly with anti-*miR-132* or its scrambled control. Anti-*miR-132* injection completely inhibited the expression of *miR-132* in the synovial membrane of the AIA mice (Fig. 4A), demonstrating the efficiency of the in vivo anti-*miR-132* treatment. The inflammatory arthritis was markedly attenuated by the injection of anti-*miR-132* as evidenced by the reduction in the joint swelling (Fig. 4B) and the histopathological scores of the joints (Fig. 4C). In further experiments, AIA mice were exposed to CS and injected with anti-*miR-132* or the scrambled control. Histological analysis of the femur-tibial joints revealed a marked increase of TRAP⁺ periarticular cells in mice exposed to CS. This increase was completely abolished by the injection of anti-*miR-132* (Fig. 4D). These results demonstrate

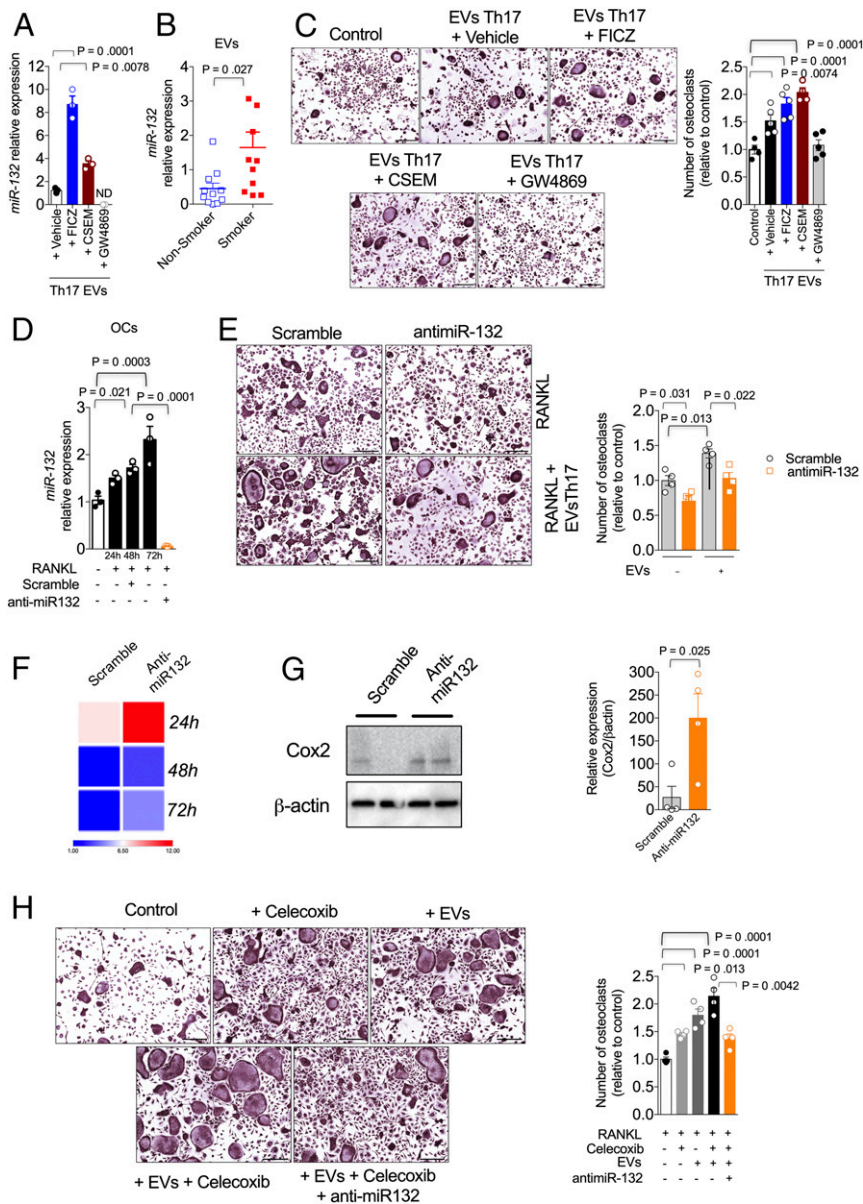


Fig. 3. AhR-induced *miR-132* is released by Th17 in extracellular vesicles and promotes osteoclastogenesis. Naive T cells ($CD4^+CD44^-CD62L^+$) were polarized to Th17 for 72 h (as in Fig. 1A) with or without FICZ, CSEM, or GW4869 (a vesicle-blocking agent). Culture supernatants were collected and EVs were isolated by ultracentrifugation. (A) Equal numbers of purified EVs were collected for qPCR analysis for *miRNA-132*. Statistical analysis was performed by one-way ANOVA followed by Bonferroni test. Data are representative of three independent experiments. ND, not detectable. (B) *miRNA-132* expression in EVs of the synovial fluids from nonsmoker ($n = 11$) and smoker ($n = 11$) RA patients. Results were calculated by the comparative threshold cycle method and are presented relative to that of *miR-361* (internal control miRNA). Statistical analysis was performed by nonparametric Mann–Whitney U test. (C) OCs were differentiated with RANKL and M-CSF in the presence of EVs from Th17 supernatants previously treated with vehicle, FICZ, CSEM, or GW4869. Images and number of TRAP⁺ multinuclear OCs are shown. (Scale bar, 75 μ m.) (D) *miR-132* expression during OC differentiation. (E) OCs were differentiated (as in C) in the presence of EVs from Th17 and transfected with anti-miR-132 or scrambled control. Images and number of TRAP⁺ multinuclear OCs are shown. (Scale bar, 75 μ m.) (F) Heatmap of *Ptgs2* expression in OCs differentiated in the presence of anti-miR-132 or scrambled control. (G) OCs collected after 72 h were analyzed by Western blot for the presence of COX2. Statistical analysis was performed by unpaired, two-tailed Student's t test. Data (mean \pm SEM) are from two independent experiments. (H) OCs were differentiated in the presence of RANKL and M-CSF for 48 h and then restimulated for 24 h with M-CSF and RANKL in the presence or absence of EVs isolated from Th17 pretreated with CSEM or a COX2 inhibitor, celecoxib. Some cells were also transfected with anti-miR-132. Representative images and number of multinuclear TRAP⁺ OCs are shown. (Scale bar, 75 μ m.) Statistical analysis was performed by one-way ANOVA followed by Bonferroni test or unpaired, two-tailed Student's t test ($n \geq 3$ /group). Data (mean \pm SEM) are representative of two independent experiments.

that the exacerbated arthritic inflammation and osteoclastogenesis induced by CS is dependent on *miR-132*.

Discussion

CS is an important environmental factor influencing a range of diseases (34). In this report, we reveal a hitherto unrecognized

mechanism by which CS may exacerbate RA (Fig. 4E). CS acts as an important agonist for AhR on Th17 cells to induce the expression of *miR-132*. The *miR-132* thus induced is packaged in EVs secreted by the activated Th17 cells. The *miR-132* in EVs then activates osteoclastogenesis by suppressing the transcription of *Ptgs2* and the expression of COX2 that would otherwise

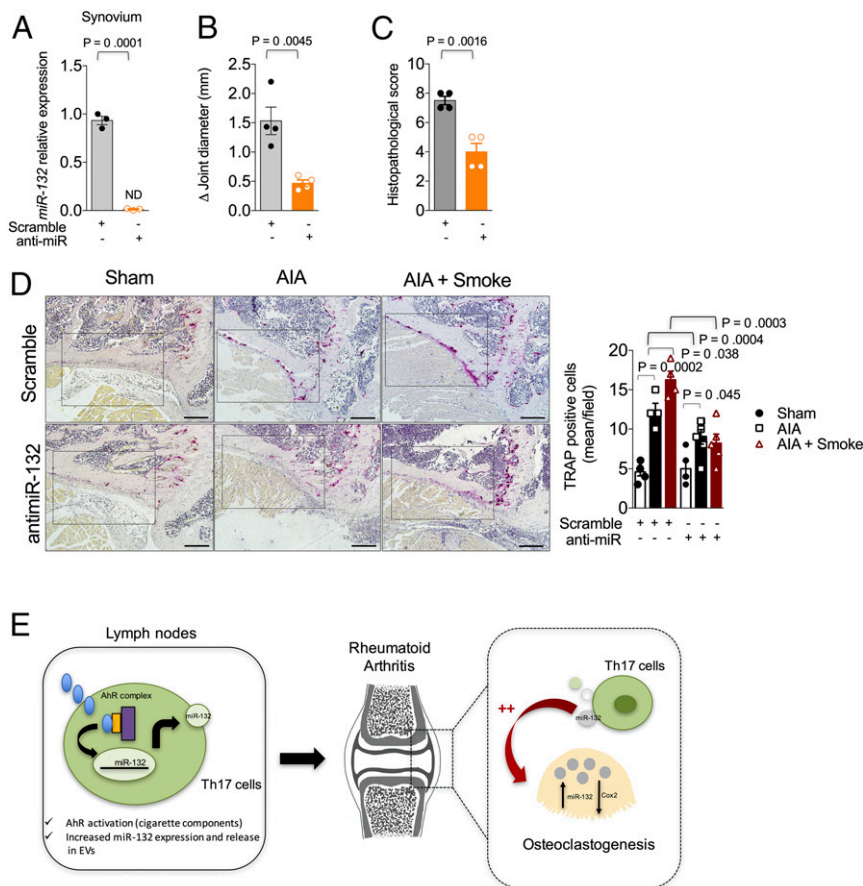


Fig. 4. Anti-miR-132 blocks arthritis and osteoclastogenesis in vivo. (A) *MIR-132* expression in the total synovial membrane of AIA mice injected intra-articularly with PBS (sham), miRCURY LNA, anti-miR-132, or scrambled control. ND, not detectable. Inflammatory arthritis of AIA mice (treated as in A) was measured as Δ joint diameter (B) and histopathological score (C). (D) AIA mice were exposed to CS and injected intra-articularly with anti-miR-132 or scrambled control. Images and number of periarticular TRAP⁺ cells in the femur-tibial joint are shown. (Scale bar, 200 μ m.) Statistical analysis was performed by one-way ANOVA followed by Bonferroni test or unpaired, two-tailed Student's *t* test. Data are mean \pm SEM, representative of two independent experiments ($n \geq 3$ /group). (E) Schematic representation of the regulation and function of *miR-132* on osteoclastogenesis in RA.

catalyze arachidonic acid to PGs, which have been documented to inhibit osteoclastogenesis (29–33). The result would be the promotion of joint destruction, an event with irreversible consequences for RA patients (35).

Nakahama et al. (36) reported that the miRNA-132/212 cluster was up-regulated by AHR activation under Th17-inducing conditions and that deficiency of this cluster prevented the enhancement of Th17 differentiation by AHR activation. Surprisingly, we could not observe an intrinsic effect of *miR-132* in Th17 cell differentiation or activation. The apparent discrepancy between our findings may be that miRNAs other than *miR-132* in the miRNA-132/212 cluster are important in the Th17 differentiation. Instead, we found that induced *miR-132* was packaged into Th17-derived EVs. T cells are known to release EVs upon activation; however, the importance of vesicular miRNAs in modulating the immune response by these cells has been little explored (37–39). Here we demonstrate that EV containing *miR-132* strongly affects the differentiation of osteoclasts in vitro. The mechanism by which RNA molecules are sorted into EVs is not completely understood, but it is recognized that important molecules from the microRNA silencing complex are present in EVs and contribute to miRNA function (40, 41). Here, we detected the presence of Ago2 in the Th17 EVs, supporting the functionality of *miR-132*. However, it should be noted that, although we have demonstrated that *miRNA-132* in EVs could induce osteoclastogenesis in vitro,

further study is needed to show that they directly affect inflammatory arthritis in vivo.

The enzyme COX2 catalyzes critical steps in the synthesis of PGs from arachidonic acid, which plays important roles in bone homeostasis and in the pathophysiology of bone disease (42). The PG effects on osteoclast function are complex and somewhat contradictory, depending on the PG subtype investigated. Exogenous PGE2, for example, can stimulate osteoclast formation and bone resorption (43, 44). In contrast, PGE2 exhibits an inhibitory effect on human osteoclast cells or osteoclasts derived from spleen cultures (29–31). Exogenous PGD2 and PGF2 α also have been shown to inhibit osteoclasts function (32, 33). However, endogenous production of eicosanoids by osteoclasts on bone metabolism has not been explored. Here, we demonstrate that Celecoxib, a specific COX2 inhibitor, enhances osteoclast formation. Consistent with our results, it has been demonstrated that osteoclasts express cytosolic phospholipase A2 (cPLA2), which is responsible for the liberation of arachidonic acid from cellular membrane and subsequent eicosanoid biosynthesis. Pharmacological inhibition of cPLA2 increased osteoclastogenesis (45), suggesting that its activity and subsequent metabolites would exert a negative control of osteoclast function. The precise mechanism of COX2 modulation of endogenous PGs in osteoclastogenesis and its functional role in vivo remains to be explored.

Our finding in the murine arthritic models appears to be applicable to clinical RA. CD4⁺ T cells from the peripheral blood of the RA patients expressed significantly higher levels of *miR-132* compared to that of the cells from the healthy controls. Furthermore, CD4⁺ T cells from the smoker RA patients expressed a significantly higher level of *miR-132* than that of the cells from the nonsmokers. Moreover, the EVs from smoker RA patients expressed significantly higher levels of *miR-132* than those from the nonsmoker RA patients. Together, these results demonstrate that AhR-induced *miR-132* in the EVs is closely associated with clinical RA. It would be important to further explore *miR-132* as a therapeutic target to alleviate inflammation and bone damage in RA.

Materials and Methods

Induction of Arthritis in Mice. Male C57BL/6, DBA/1J, and *Ahr*^{-/-} mice were bred in a specific-pathogen-free animal facility at the School of Medicine of Ribeirão Preto, University of São Paulo, Brazil. All experiments were performed in accordance with the guidelines outlined by Standing Committee on Animals at Ribeirão Preto Medical School, University of São Paulo (no. 048/2012). *Ahr*^{-/-} mice on the C57BL/6 background were provided by Frank Gonzalez, National Cancer Institute, NIH, Bethesda, MD. For induction of AIA, C57BL/6 mice were injected subcutaneously with methylated bovine serum albumin in complete Freund adjuvant (CFA) and boosted with the same preparation in incomplete Freund adjuvant (IFA). For CIA, DBA/1J mice were injected intradermally with bovine type II collagen in CFA. Detailed information describing protocols for T cell differentiation, osteoclast cultures, microarrays, flow cytometry, extracellular vesicle purification and analysis, anti-MiR transfections, and cigarette smoke exposure is provided in *SI Appendix*.

Patients and Healthy Donors. Peripheral blood samples from 37 RA patients and 34 healthy individuals were obtained from CD4⁺ T cell analysis. All patients fulfilled the 2010 American College of Rheumatology and European League against rheumatism criteria for RA classification (46) and did not receive any treatment. Disease activity was measured by the Disease Activity Score, including a 28-joint count, and RA patients were stratified according to smoking in smokers and nonsmokers. Synovial liquid from 22 RA patients was also collected for isolation of extracellular vesicles. The clinical features of the subjects are detailed *SI Appendix, Table S2*. All donors provided informed consent to participate in the study, which was approved by the Research Ethics Committee of Ribeirão Preto Medical School Hospital (HCFMRP)–University of São Paulo (Protocol 5776/2015). Subjects presenting other autoimmune or rheumatic diseases and infectious disorders or that were serologically positive for Chagas disease, hepatitis B and C, or HIV were excluded. All laboratory analyses of the samples were performed blind to the donor status. Further information is provided in *SI Appendix*.

Data Availability. Microarray data analysis data have been deposited in the Gene Expression Omnibus database ([GSE149169](https://www.ncbi.nlm.nih.gov/geo/query/acc.cgi?acc=GSE149169)).

ACKNOWLEDGMENTS. We thank Sergio L. C. Almeida, Patricia Rolim, and members of the Rheumatoid Arthritis team for their advice and clinical assistance; Dr. Fausto Almeida research group for support with Nanosight analysis; Ieda R. S. Schivo, Sergio R. Rosa, Ana Katia dos Santos, Denise Ferraz, and Tadeu F. Vieira (in memory) for technical assistance. This work was supported by grants from the São Paulo Research Foundation (FAPESP, 2012/02438-0 and 2013/08216-2 Center for Research in Inflammatory Disease) and from the University of São Paulo (NAP-DIN, 11.1.21625.01.0).

- G. S. Firestein, Evolving concepts of rheumatoid arthritis. *Nature* **423**, 356–361 (2003).
- I. B. McInnes, G. Schett, The pathogenesis of rheumatoid arthritis. *N. Engl. J. Med.* **365**, 2205–2219 (2011).
- J. S. Smolen *et al.*, Rheumatoid arthritis. *Nat. Rev. Dis. Primers* **4**, 18001 (2018).
- H. Källberg *et al.*; EIRA Study Group, Smoking is a major preventable risk factor for rheumatoid arthritis: Estimations of risks after various exposures to cigarette smoke. *Ann. Rheum. Dis.* **70**, 508–511 (2011).
- J. Sokolove *et al.*, Increased inflammation and disease activity among current cigarette smokers with rheumatoid arthritis: A cross-sectional analysis of US veterans. *Rheumatology (Oxford)* **55**, 1969–1977 (2016).
- Y. Ishikawa, C. Terao, The impact of cigarette smoking on risk of rheumatoid arthritis: A narrative review. *Cells* **9**, 475 (2020).
- M. S. Denison, S. R. Nagy, Activation of the aryl hydrocarbon receptor by structurally diverse exogenous and endogenous chemicals. *Annu. Rev. Pharmacol. Toxicol.* **43**, 309–334 (2003).
- L. Stejskalova, Z. Dvorak, P. Pavek, Endogenous and exogenous ligands of aryl hydrocarbon receptor: Current state of art. *Curr. Drug Metab.* **12**, 198–212 (2011).
- J. Talbot *et al.*, Smoking-induced aggravation of experimental arthritis is dependent of aryl hydrocarbon receptor activation in Th17 cells. *Arthritis Res. Ther.* **20**, 119 (2018).
- B. Stockinger, P. Di Meglio, M. Gialitakis, J. H. Duarte, The aryl hydrocarbon receptor: Multitasking in the immune system. *Annu. Rev. Immunol.* **32**, 403–432 (2014).
- M. Veldhoen *et al.*, The aryl hydrocarbon receptor links TH17-cell-mediated autoimmunity to environmental toxins. *Nature* **453**, 106–109 (2008).
- Y. Z. Gu, J. B. Hogenesch, C. A. Bradfield, The PAS superfamily: Sensors of environmental and developmental signals. *Annu. Rev. Pharmacol. Toxicol.* **40**, 519–561 (2000).
- M. Adachi *et al.*, Cigarette smoke condensate extracts induce IL-1 β production from rheumatoid arthritis patient-derived synoviocytes, but not osteoarthritis patient-derived synoviocytes, through aryl hydrocarbon receptor-dependent NF- κ B activation and novel NF- κ B sites. *J. Interferon Cytokine Res.* **33**, 297–307 (2013).
- S. Kobayashi *et al.*, A role for the aryl hydrocarbon receptor and the dioxin TCDD in rheumatoid arthritis. *Rheumatology (Oxford)* **47**, 1317–1322 (2008).
- F. J. Quintana *et al.*, Control of T(reg) and T(H)17 cell differentiation by the aryl hydrocarbon receptor. *Nature* **453**, 65–71 (2008).
- A. Kimura, T. Naka, K. Nohara, Y. Fujii-Kuriyama, T. Kishimoto, Aryl hydrocarbon receptor regulates Stat1 activation and participates in the development of Th17 cells. *Proc. Natl. Acad. Sci. U.S.A.* **105**, 9721–9726 (2008).
- T. Nakahama *et al.*, Aryl hydrocarbon receptor deficiency in T cells suppresses the development of collagen-induced arthritis. *Proc. Natl. Acad. Sci. U.S.A.* **108**, 14222–14227 (2011).
- I. Ivanov *et al.*, The orphan nuclear receptor ROR γ directs the differentiation program of proinflammatory IL-17⁺ T helper cells. *Cell* **126**, 1121–1133 (2006).
- K. Sato *et al.*, Th17 functions as an osteoclastogenic helper T cell subset that links T cell activation and bone destruction. *J. Exp. Med.* **203**, 2673–2682 (2006).
- N. Komatsu *et al.*, Pathogenic conversion of Foxp3⁺ T cells into TH17 cells in autoimmune arthritis. *Nat. Med.* **20**, 62–68 (2014).
- V. Ambros, The functions of animal microRNAs. *Nature* **431**, 350–355 (2004).
- B. M. Engels, G. Hutvagner, Principles and effects of microRNA-mediated post-transcriptional gene regulation. *Oncogene* **25**, 6163–6169 (2006).
- K. M. Pauley *et al.*, Upregulated miR-146a expression in peripheral blood mononuclear cells from rheumatoid arthritis patients. *Arthritis Res. Ther.* **10**, R101 (2008).
- K. Murata *et al.*, Plasma and synovial fluid microRNAs as potential biomarkers of rheumatoid arthritis and osteoarthritis. *Arthritis Res. Ther.* **12**, R86 (2010).
- R. M. O'Connell, D. S. Rao, A. A. Chaudhuri, D. Baltimore, Physiological and pathological roles for microRNAs in the immune system. *Nat. Rev. Immunol.* **10**, 111–122 (2010).
- R. M. Johnstone, Exosomes biological significance: A concise review. *Blood Cells Mol. Dis.* **36**, 315–321 (2006).
- H. Valadi *et al.*, Exosome-mediated transfer of mRNAs and microRNAs is a novel mechanism of genetic exchange between cells. *Nat. Cell Biol.* **9**, 654–659 (2007).
- L. de la Rica *et al.*, NF- κ B-direct activation of microRNAs with repressive effects on monocyte-specific genes is critical for osteoclast differentiation. *Genome Biol.* **16**, 2 (2015).
- K. Ono *et al.*, Biphasic effect of prostaglandin E2 on osteoclast formation in spleen cell cultures: Role of the EP2 receptor. *J. Bone Miner. Res.* **20**, 23–29 (2005).
- T. Shibata-Mozaki *et al.*, Endogenous prostaglandin E2 inhibits aberrant overgrowth of rheumatoid synovial tissue and the development of osteoclast activity through EP4 receptor. *Arthritis Rheum.* **63**, 2595–2605 (2011).
- I. Take *et al.*, Prostaglandin E2 strongly inhibits human osteoclast formation. *Endocrinology* **146**, 5204–5214 (2005).
- M. Durand, M. A. Gallant, A. J. de Brum-Fernandes, Prostaglandin D2 receptors control osteoclastogenesis and the activity of human osteoclasts. *J. Bone Miner. Res.* **23**, 1097–1105 (2008).
- X. Xu *et al.*, The prevention of latanoprost on osteoclastogenesis in vitro and lipopolysaccharide-induced murine calvaria osteolysis in vivo. *J. Cell. Biochem.* **119**, 4680–4691 (2018).
- C. Perricone *et al.*, Smoke and autoimmunity: The fire behind the disease. *Autoimmun. Rev.* **15**, 354–374 (2016).
- G. Schett, E. Gravallese, Bone erosion in rheumatoid arthritis: Mechanisms, diagnosis and treatment. *Nat. Rev. Rheumatol.* **8**, 656–664 (2012).

36. T. Nakahama *et al.*, Aryl hydrocarbon receptor-mediated induction of the microRNA-132/212 cluster promotes interleukin-17-producing T-helper cell differentiation. *Proc. Natl. Acad. Sci. U.S.A.* **110**, 11964–11969 (2013).
37. M. Mittelbrunn *et al.*, Unidirectional transfer of microRNA-loaded exosomes from T cells to antigen-presenting cells. *Nat. Commun.* **2**, 282 (2011).
38. I. S. Okoye *et al.*, MicroRNA-containing T-regulatory-cell-derived exosomes suppress pathogenic T helper 1 cells. *Immunity* **41**, 503 (2014).
39. L. N. Ventimiglia, M. A. Alonso, Biogenesis and function of T cell-derived exosomes. *Front. Cell Dev. Biol.* **4**, 84 (2016).
40. J. Guduric-Fuchs *et al.*, Selective extracellular vesicle-mediated export of an overlapping set of microRNAs from multiple cell types. *BMC Genomics* **13**, 357 (2012).
41. S. A. Melo *et al.*, Cancer exosomes perform cell-independent microRNA biogenesis and promote tumorigenesis. *Cancer Cell* **26**, 707–721 (2014).
42. K. A. Blackwell, L. G. Raisz, C. C. Pilbeam, Prostaglandins in bone: Bad cop, good cop? *Trends Endocrinol. Metab.* **21**, 294–301 (2010).
43. H. Kaji *et al.*, Prostaglandin E2 stimulates osteoclast-like cell formation and bone-resorbing activity via osteoblasts: Role of cAMP-dependent protein kinase. *J. Bone Miner. Res.* **11**, 62–71 (1996).
44. X. Y. Tian *et al.*, Continuous infusion of PGE2 is catabolic with a negative bone balance on both cancellous and cortical bone in rats. *J. Musculoskelet. Neuronal Interact.* **7**, 372–381 (2007).
45. H. Allard-Chamard, P. Dufort, S. Haroun, A. J. de Brum-Fernandes, Cytosolic phospholipase A2 and eicosanoids modulate life, death and function of human osteoclasts in vitro. *Prostaglandins Leukot. Essent. Fatty Acids* **90**, 117–123 (2014).
46. D. Aletaha *et al.*, 2010 rheumatoid arthritis classification criteria: An American College of Rheumatology/European League against rheumatism collaborative initiative. *Arthritis Rheum.* **62**, 2569–2581 (2010).